

PROPERTIES OF SQUEEZE CAST MgZnAl AND MGZnAlCA ALLOYS WITH ICOSAHEDRAL PHASE DURING ANNEALING WITH CONSTANT HEATING RATES

KODETOVÁ Veronika, VLACH Martin, STULÍKOVÁ Ivana, SMOLA Bohumil, KEKULE Tomáš

Charles University in Prague, Faculty of Mathematics and Physics, Prague, Czech Republic, EU

Abstract

The Mg-11.5wt.%Zn-3.0wt.%Al and Mg-5.1wt.%Zn-3.3wt.%Al-0.1wt.%Ca alloys were squeeze cast under a protective gas atmosphere (Ar + 1% SF₆). Precipitation reactions were studied by differential scanning calorimetry at heating rates of 0.5 - 30 K/min. Electrical resistometry at 78 K and microhardness (HV0.5) at room temperature were performed additionally. The specimens were subjected to isochronal annealing with steps of 20 K/20 min up to 300 °C. The thermal measurements revealed two exothermic effects during linear heat treatment in the temperature range of 100 - 250 °C at heating rates of 2 - 30 K/min. In agreement to the thermal response, two stages of electrical resistivity decrease were observed in the same temperature range. The lower thermal and absolute resistivity changes were observed in the alloy with Ca-addition. Activation energies obtained from the thermal measurements using the Kissinger method for the two mentioned processes were calculated as $Q_1 = (124 \pm 17) \text{ kJ} \cdot \text{mol}^{-1}$ and $Q_2 = (133 \pm 4) \text{ kJ} \cdot \text{mol}^{-1}$ in both alloys.

Keywords: Differential scanning calorimetry, electrical resistometry, activation energy, icosahedral phase

1. INTRODUCTION

Magnesium alloys exhibit low density, high specific strength and they are being increasingly applied in aircraft, electronic industries and in automotive industry in order to save mass thereby reducing fuel consumption and pollution [1-3]. The addition of zinc to magnesium can lower the corrosion rates of the alloys and improve mechanical properties [2]. Commonly used magnesium alloys on Mg-Al based system have excellent castability, low cost and good mechanical properties. However there is a limitation to temperature below 120 °C because of poor heat resistance [1]. Magnesium alloys show attractive properties for biomaterial applications, too. Studies on Mg-Zn-Ca have shown that this alloy has a very good biocompatibility [4, 5].

Icosahedral phase in Mg alloys exhibits very good strengthening properties [6-9]. The formation of icosahedral phase has been considered as one of the most effective methods for expansion of high strength lightweight Mg alloys to aerospace and automotive industry [9, 10]. This phase was found in Mg-Zn-Al, Mg-Cu-Al or in Mg-Zn-Y alloys [6-8]. Quasicrystals have many interesting properties such as very high hardness, thermal stability and low electrical conductivity at room temperature or high corrosion resistance [6-9]. The icosahedral phase particles also pin grain boundaries and retard grain growth. Icosahedral phase is metastable and transforms to the equilibrium τ phase in the as-cast Mg alloys annealed at 170 - 220 °C [10].

2. EXPERIMENTAL DETAILS

The Mg-11.5 wt.% Zn-3.0 wt.% Al and Mg-5.1 wt.% Zn-3.3 wt.% Al-0.1 wt.% Ca alloys were squeeze cast under a protective gas atmosphere (Ar + 1% SF₆). The alloys were pressed in two steps with maximal pressure 50 MPa and 150 MPa. The temperature of liquid was 750 - 850 °C.

The temperature ranges of phase transformations in the alloys were determined by electrical resistivity measurements at 78 K and by microhardness (HV0.5) measurements at room temperature after annealing in isochronal steps of 20 K/20 min. The heat treatment was undertaken in a stirred oil bath up to 240 °C and in a furnace with Ar-protective atmosphere up to 300 °C. Each step was followed by quenching. Relative electrical resistivity changes $\Delta\rho/\rho_0$ were obtained with an accuracy of 10^{-4} (ρ_0 is the value of resistivity in the initial state).

The H-shaped specimens were used for resistivity measurements. Resistivity was measured by the DC four-point method with a dummy specimen in series. The influence of parasitic thermo-electromotive force was suppressed by current reversal.

The influence of isochronal annealing on mechanical properties was studied using Vickers microhardness measurements following the same procedure as in resistivity measurements. The measurement started no longer than 5 minutes after the heat treatment step to minimise eventual natural ageing [11].

The thermal analyses of the Mg-Zn-Al-(Ca) alloys were studied using differential scanning calorimetry (DSC) performed at heating rates of 0.5, 1, 2, 5, 10, 20 and 30 K·min⁻¹ in the Netzsch DSC 200 F3 apparatus. The temperature range of the measurements was from room temperature to 300 °C. A specimen of mass between 10-20 mg was placed in Al₂O₃ crucibles. Measurements were performed without a reference specimen. Nitrogen flowed at the rate of 40 ml/min as a protective atmosphere.

Transmission electron microscopy (TEM) and electron diffraction (ED) were carried out in JOEL JEM 2000FX electron microscope to determine the microstructure of the squeeze cast alloys.

3. RESULTS AND DISCUSSION

Relative resistivity changes caused by step-by-step isochronal annealing up to 300 °C in the Mg-Zn-Al and Mg-Zn-Al-Ca alloys are shown in **Fig. 1**. The resistivity annealing curves show gradual decrease of $\Delta\rho/\rho_0$ up to ~ 220 °C followed by resistivity decrease to the minimum at ~ 280 °C in both alloys. Thereafter resistivity increases in both alloys. The initial values of electrical resistivity were measured as ~ 58 nΩ·m for the Mg-Zn-Al alloy and ~ 47 nΩ·m for the Mg-Zn-Al-Ca alloy. The difference of electrical resistivity $\Delta\rho$ between the initial state and after annealing up to 280 °C was determined as 6 nΩ·m and 3 nΩ·m for the Mg-Zn-Al and the Mg-Zn-Al-Ca alloy, respectively. Higher initial value of electrical resistivity as well as larger resistivity changes after isochronal annealing for the Mg-Zn-Al are probably caused by higher content of additives (especially zinc) in the alloy.

Fig. 2 shows the response of microhardness HV0.5 to step-by-step isochronal annealing. The initial values of microhardness were measured as (87 ± 2) for the Mg-Zn-Al and (59 ± 2) for the Mg-Zn-Al-Ca alloy, respectively. The grain size was observed as ~ 40 μm in both alloys. Thus the difference of the initial microhardness values in the alloy without Ca-addition is probably caused by higher concentration of additives, again. One can see that the isochronal annealing has a negligible effect on hardening in both alloys. At temperatures above ~ 240 °C microhardness of the alloys slowly decreases. The value of microhardness of the Mg-Zn-Al alloy at the end of annealing is below the initial value.

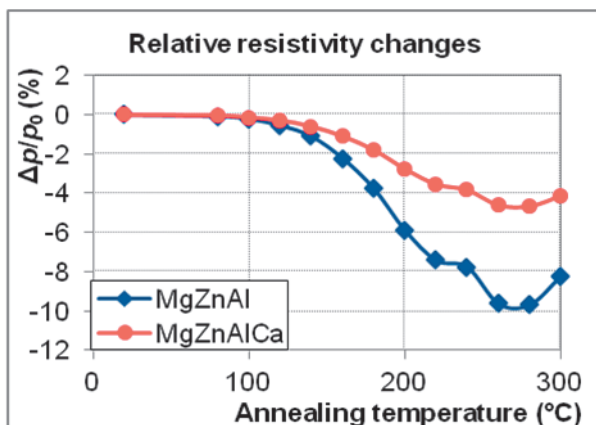


Fig. 1 Isochronal resistivity annealing curves (20 K/20 min)

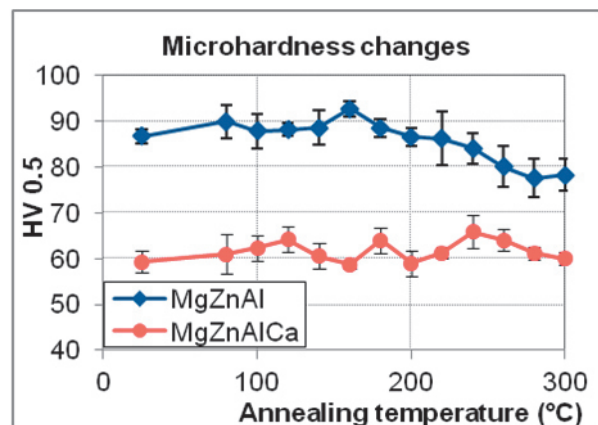


Fig. 2 Isochronal microhardness (HV0.5) annealing curves (20 K/20 min)

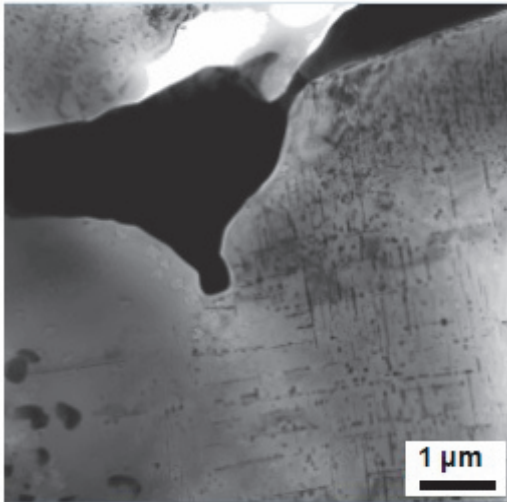


Fig. 3a TEM bright field image of the Mg-Zn-Al squeeze cast alloy. See grain boundary phase, rods and oval particles

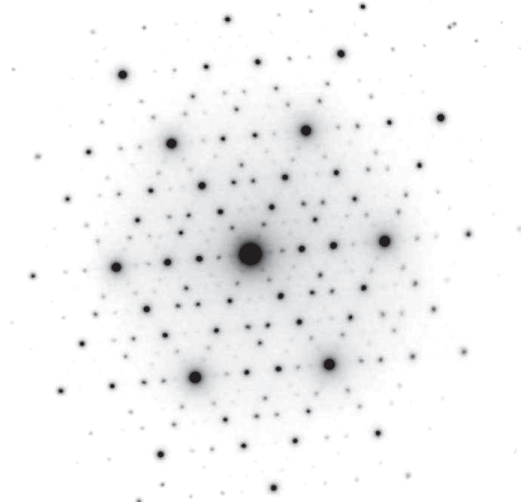


Fig. 3b ED of the grain boundary phase in the Mg-Zn-Al squeeze cast alloy identified as 3-fold symmetry zone of icosahedral phase

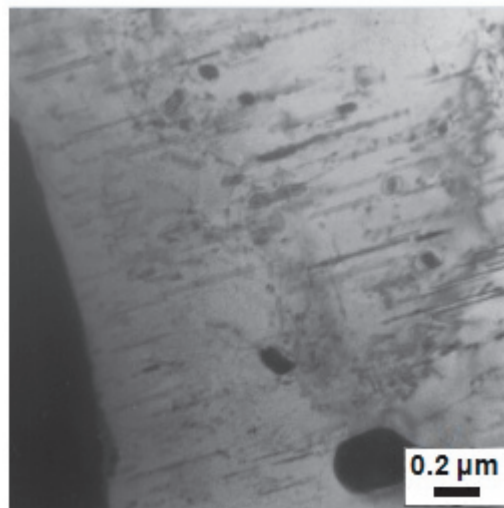


Fig. 4 TEM bright field image of the Mg-Zn-Al-Ca squeeze cast alloy

The microstructures in the initial state are shown in **Figs. 3** and **4**. TEM proved an existence of grain boundary phases in both alloys. This phase was identified using ED as icosahedral phase in the Mg-Al-Zn alloy (see **Fig. 3b**). The phase contains Mg, Zn and Al and the concentration is enclosed to the composition of the icosahedral phase described in [12]. Grain boundary regions were less occupied by icosahedral phase in the alloy with Ca-addition. It is probably caused by lower concentration of zinc. The volume fraction of the grain boundary phase is also lower in the Mg-Zn-Al-Ca alloy.

A high density of rods (size of 140 - 550 nm) perpendicular to basal plane and fine coherent oval particles (size of 20 - 55 nm) were observed inside α -Mg phase grains in both alloys. The morphology of these phases is closed to the phases observed in binary Mg-Zn alloys [13, 14]. A higher density of fine oval particles was observed in the Mg-Zn-Al than in the Mg-Zn-Al-Ca alloy. Coarse block particles (size of 50 -120 nm) were detected only in the Mg-Zn-Al-Ca alloy. Unfortunately we have no clear information about structure of these phases.

Negative numerical derivatives of the measured resistivity annealing curves from Fig. 1 are plotted in Figs. 5a and 5b for a better recognition. The obtained spectrum can be fitted by Gaussian curves using the method of least squares [15]. The first positive stage in both alloys is composed of three sub-stages with maxima at ~120 °C, ~160 °C and ~200 °C. The second positive stage (Fig. 5) in both studied alloys has maximum at ~250 °C.

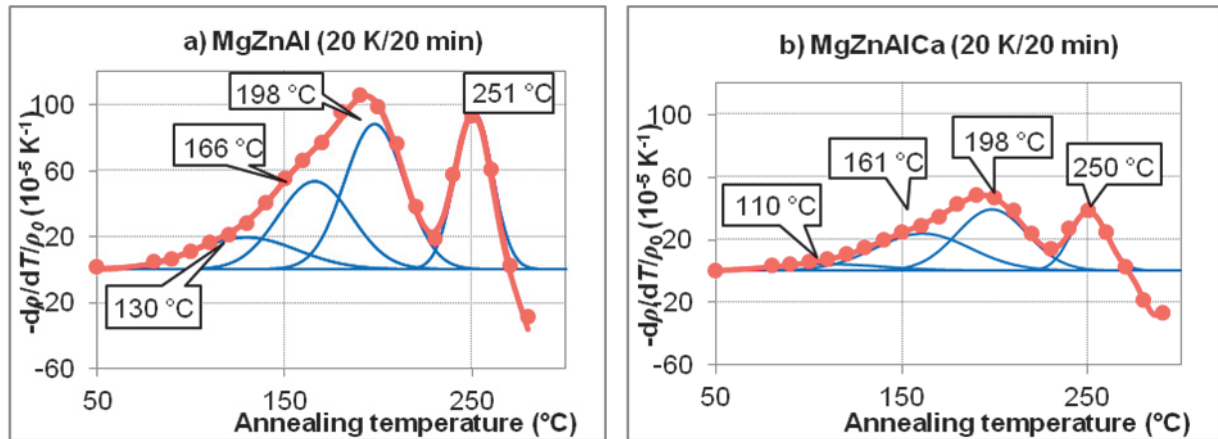


Fig. 5 Spectra derived as negative derivative of the isochronal resistivity-annealing curves fitted by Gaussian curves. The initial value of electrical resistivity is ρ_0 . a) Mg-Zn-Al alloy, b) Mg-Zn-Al-Ca alloy

Differential scanning calorimetry of both alloys revealed three exothermic effects (labelled as effect 1, 2 and 3) at heating rate of 1 K/min. However, DSC measurements revealed only two exothermic effects (effect 1, effect 2) at higher heating rates (2 - 30 K/min) in both alloys. No thermal changes were detected in DSC curves at heating rate 0.5 K/min. For illustration, Fig. 6 shows DSC curve of Mg-Zn-Al at heating rate of 1 K/min. There are three exothermic stages fitted by Gaussian curves. It is seen that exothermic peaks (effect 1 and 2) correspond to the temperature position of the positive resistivity spectra sub-stages in Fig. 5a.

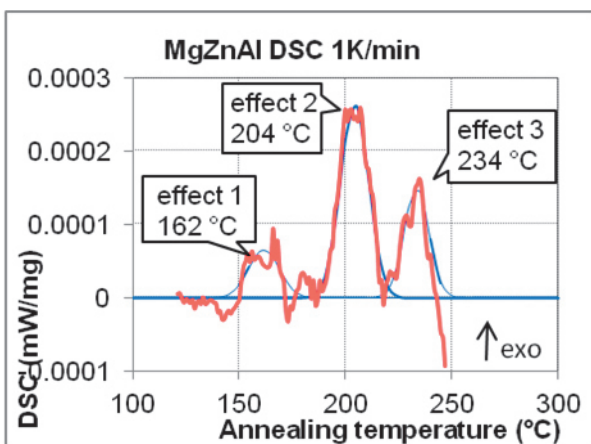


Fig. 6 DSC trace (red line) at heating rate 1 K/min of the Mg-Zn-Al alloy fitted up to 250 °C by Gaussian curves (blue lines)

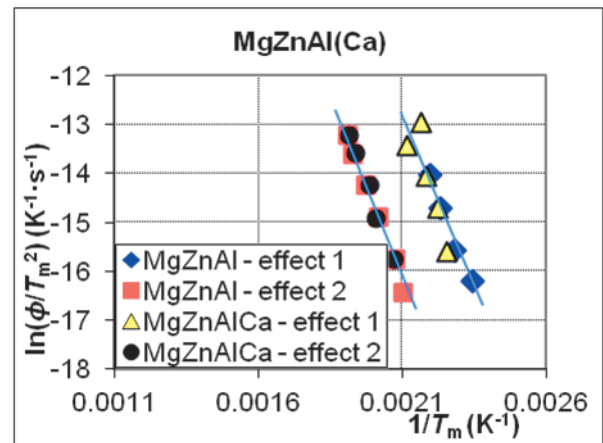


Fig. 7 Kissinger plot of exothermic heat effects in the squeeze-cast Mg-Zn-Al-(Ca) alloys. ϕ is the linear heating rate; T_m is the peak temperature of DSC trace for particular exothermic heat effect

No exothermic effect was detected after annealing up to ~ 140 °C for any heating rate. The third exothermic stage (effect 3) with maximum at ~ 235 °C in DSC curve in Fig. 6 corresponds to the resistivity spectra stage with maximum at ~ 250 °C. The temperature position of the heat flow peaks (effect 1 and 2) shifts to higher temperatures with increasing heating rates. The lower thermal changes were observed in the alloy with Ca-addition, it agrees very well with the lower resistivity changes in the alloy with Ca-addition.

The Kissinger method [16] with the assumption that the peak temperature T_m in DSC curves for individual precipitation effects can be expressed as

$$\ln\left(\frac{\Phi}{T_m^2}\right) = -\frac{Q}{RT_m} + C \quad (1)$$

where C is a constant, Q the process activation energy, R the gas constant, Φ the heating rate.

Fig. 7 shows the Kissinger plot in the coordinate system of $[\ln(\Phi/T_m^2); 1/T_m]$ for the Mg-Zn-Al and Mg-Zn-Al-Ca alloys together. The Kissinger plot shows that maxima of the two exothermic effects (effect 1 and 2) observed at DSC curves up to 250 °C were detected at the same temperatures in both alloys. The Ca-addition does not influence the exothermic processes in DSC measurements. Activation energies of the two processes were calculated by the Kissinger method as $Q_1 = (124 \pm 17) \text{ kJ}\cdot\text{mol}^{-1}$ and $Q_2 = (133 \pm 4) \text{ kJ}\cdot\text{mol}^{-1}$ in both alloys.

Preliminary TEM and ED results proved neither changes of volume fraction nor composition of boundary phases after annealing up to 240 °C. Volume fraction of the fine coherent oval particles increases after annealing up to 240 °C in both alloys compared to the initial state. However, the thorough additional microstructure observation is needed. With respect to the thermal changes, electrical resistivity and microhardness changes up to ~ 250 °C we suppose that they are mainly caused by precipitation and/or coarsening of particles inherent to Mg-Zn system.

4. CONCLUSIONS

Microstructure observation proved existence of grain boundary phases in the squeeze cast Mg-Zn-Al-(Ca) alloys. This phase was identified by selective electron diffraction as an icosahedral phase. Three exothermic processes were observed by DSC measurements in the alloys. The third process was observed only at heating rate of 1 K/min. Thus the activation energies were calculated only for the two exothermic processes by the Kissinger method as $Q_1 = (124 \pm 17) \text{ kJ}\cdot\text{mol}^{-1}$ and $Q_2 = (133 \pm 4) \text{ kJ}\cdot\text{mol}^{-1}$ in both alloys. The processes are probably caused by precipitation and/or coarsening of particles of the Mg-Zn system. The results obtained by electrical resistometry correspond very well to DSC measurements. The lower thermal and resistivity changes were observed in the alloy with Ca-addition. No influence of Ca-addition on maxima of the exothermic processes up to 250 °C was observed in DSC measurements. The difference of initial microhardness values in both alloys is probably caused by different concentrations of additives, especially of zinc.

ACKNOWLEDGEMENTS

The research leading to these results has received funding from the People Programme (Marie Curie Actions) of the European Union's Seventh Framework Programme FP7/2007-2013/ under REA grant agreement No. 289163.

REFERENCES

- [1] VAN X., NI H., HUANG M., ZHANG H., SUN J. Microstructure, mechanical properties and creep resistance of Mg-(8%-12%)Zn-(2%-6%)Al alloys. *Trans. Nonferrous Met. Soc. China*, Vol. 23, 2013, pp. 896-903, doi. 10.1016/S1003-6326(13)62814-9.
- [2] HOMAYUN B., AFSHAR A. Microstructure, mechanical properties, corrosion behaviour and cytotoxicity of Mg-Zn-Al-Ca alloys as biodegradable materials. *Journal of Alloys and Compounds*, Vol. 607, 2014, Issue 10, pp. 1-10, doi. 10.1016/j.jallcom.2014.04.059.
- [3] ZHANG J., LI Z., GUO Z., PAN F. Solidification microstructural constituent and its crystallographic morphology of permanent-mould-cast Mg-Zn-Al alloys, *Trans. Nonferrous Met. Soc. China*, Vol. 16, 2006, pp. 452-458, doi. 10.1016/S1003-6326(06)60077-0.

- [4] SUN Y., ZHANG B., WANG Y., GENG L., JIAO X. Preparation and characterization of a new biomedical Mg-Zn-Ca alloy. *Mater. Des.*, Vol. 34, 2012, pp. 58-64, doi. 10.1016/j.matdes.2011.07.058.
- [5] XIA Y., ZHANG B., WANG Y., QIAN M., GENG L. In-vitro cytotoxicity and in vivo biocompatibility of as-extruded Mg-4.0Zn-0.2Ca alloy. *Mater. Sci. Eng. C*, Vol. 32, 2012, Issue 4, pp. 665-669, doi. 10.1016/j.msec.2012.01.004.
- [6] SINGH A., WATANABE M., KATO A., TSAI A.P. Strengthening in magnesium alloys by icosahedral phase. *Science and Technology of Advances Materials*, Vol. 6, 2005, pp. 895-901, doi. 10.1016/j.stam.2005.08.005.
- [7] XU D.K., HAN E.H. Effects of icosahedral phase formation on the microstructure and mechanical improvement of Mg alloys: A review. *Progress in Natural Science: Materials International*, Vol. 22, Issue 5, 2012, pp. 364-385, doi. 10.1016/j.pnsc.2012.09.005.
- [8] WAN X., NI H., HUANG M., ZHANG H., SUN J. Microstructure, mechanical properties and creep resistance of Mg-(8%-12%)Zn-(2%-6%)Al alloys. *Trans. Nonferrous Met. Soc. China*, Vol. 23, 2013, pp. 896-903, doi. 10.1016/S1003-6326(13)62545-5.
- [9] ZHANG J., ZUO R., CHEN Y., PAN F., LUO X. Microstructure evolution during homogenization of a τ -type Mg-Zn-Al alloy. *Journal of Alloys and Compounds*, Vol. 448, 2008, pp. 316-320, doi. 10.1016/j.jallcom.2006.10.135.
- [10] VOGEL M., KRAFT O., ARZT E. Creep behaviour of magnesium die-cast alloy ZA85. *Scripta Mater*, Vol. 48 Issue 8, 2003, pp. 985-990, doi. 10.1016/S1359-6462(02)00588-2.
- [11] BUHA J., OHKUBO T. Natural Aging in Mg-Zn(-Cu) Alloys. *Metallurgical and Materials Transactions A*, Vol. 39 Issue 9, 2008, pp. 2259-2273, doi. 10.1007/s11661-008-9545-y.
- [12] XIAOFENG W., YANGSHAN S., FENG X., JING B., WEIJIAN T. Effects of Sc and Ca on the microstructure and properties of Mg-12Zn-4Al-0.3Mn alloy. *Materials Science and Engineering A*, Vol. 508, 2009, pp. 50-58, doi.10.1016/j.msea.2008.12.046.
- [13] HRADILOVÁ M., VOJTĚCH D., KUBÁSEK J., ČAPEK J., VLACH M. Structural and mechanical characteristics of Mg-4Zn and Mg-4Zn-0.4Ca alloys after different thermal and mechanical processing routes. *Materials Science & Engineering*, Vol. A 586, 2013, pp. 284-291, doi. 10.1016/j.msea.2013.08.008.
- [14] ČÍŽEK J., PROCHÁZKA I., SMOLA B., STULÍKOVÁ I., VLACH M., OČENÁŠEK V., KULYASOVA O.B., ISLAMGALIEV R.K. Precipitation effects in ultra-fine-grained Mg-RE alloys. *International Journal of Materials Research*, Vol. 100, Issue 6, 2009, pp. 780-784, doi. 10.3139/146.110103.
- [15] STULÍKOVÁ, I., SMOLA, B. Identification and characterization of phase transformations by the resistivity measurements in Mg-RE-Mn alloys. *Solid State Phenomena*, Vol. 138, 2008, pp. 57-62, doi. 10.4028/www.scientific.net/SSP.138.57.
- [16] STARINK, M.J. The determination of activation energy from linear heating rate experiments: A comparison of the accuracy of isoconversion methods. *Thermochimica Acta*, Vol. 404, Issues 1-2, 2003, pp.163-176, doi. 10.1016/S0040-6031(03)00144-8.